Inorganic Chemistry

Article

pubs.acs.org/IC

Intramolecular Aminoalkene Hydroamination Mediated by a Tethered Bis(ureate)zirconium Complex: Computational Perusal of Various Pathways for Aminoalkene Activation

Sven Tobisch*

School of Chemistry, University of St Andrews, Purdie Building, North Haugh, St Andrews KY16 9ST, United Kingdom

Supporting Information

ABSTRACT: The present study comprehensively explores alternative mechanistic pathways for the intramolecular hydroamination of the prototype 2,2-dimethyl-5-penten-1-amine aminoalkene (**1**) by bis(ureate)$Zr^{IV}(NMe_2)_2(HNMe_2)$ (**2**), which proceeds through a $Zr^{IV}(NHR)_2$ intermediate using density functional theory (DFT) calculations. The classical stepwise σ-insertive mechanism that includes insertion of the C=C double bond into the Zr−N amido σ bond followed by Zr−C alkyl-bond aminolysis has been compared with a single-step pathway for amidoalkene → cycloamine conversion through a concerted amino proton transfer associated with N−C ring closure. Noncompetitive kinetics for reversible σ-insertive cyclization, together with the incompatibility of a turnover-limiting insertion step with observed pronounced primary kinetic isotope effects (KIEs), strongly militates against the operation of a σ-insertive mechanism. A noninsertive pathway evolving through an ordered six-center transition-state structure describing N−C bond formation at an axial Zr−N amido σ bond triggered by concurrent proton transfer from an equatorially bound substrate molecule onto the adjacent olefin−carbon center is found to prevail energetically. The proton-triggered noninsertive cyclization commencing from a catalytically relevant $Zr^{IV}(NHR)_2(NH_2R)$ substrate adduct is strongly downhill, followed by product expulsion via dissociative amine exchange. The assessed effective barrier compares reasonably well with the previously determined Eyring parameters, and the computationally estimated primary KIEs match the observed values pleasingly well. The present study reveals a comparable strength of substrate and product binding in relevant seven-coordinate intermediates, together with a rapid equilibrium between related primary and secondary amido species, which favors the former, as unique features of the studied catalyst. Thus, in line with experimental observations, competitive product inhibition can be discarded. On the basis of all of these findings, it is suggested that a $Zr(NHR)_2$(substrate) intermediate corresponds to the catalyst resting state at high substrate concentrations, while it becomes a $Zr(NHR)_2$(cycloamine) species when the product concentration is high or with the addition of excess 2-methylpiperidine, and this ambivalent behavior explains the observed operation of two distinct kinetic regimes, depending upon the extent of the reaction.

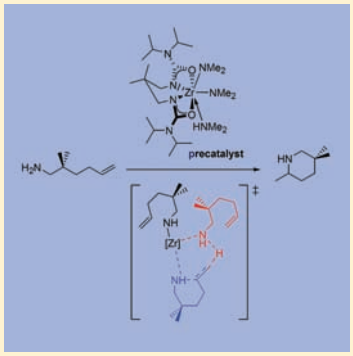

INTRODUCTION

Catalytic hydroamination (HA), the direct addition of a N−H bond across an unsaturated C−C linkage, allows facile and atom-economical access to industrially relevant organonitrogen commodity and fine chemicals.[1] The intramolecular HA/cyclization constitutes a particularly powerful and concise route to functionalized nitrogen heterocycles. Significant research efforts over the last 2 decades have led to the discovery of efficient group 4 metal-based catalysts. Given their synthetic versatility, together with low environmental impact and economic viability, titanium and zirconium compounds appear as particularly promising catalysts. Further catalyst development, however, critically relies on a precise knowledge of the operative mechanistic pathway.

Three distinct mechanistic pathways have emerged over the years as a result of comprehensive mechanistic exploration conducted by various groups. Neutral group 4 metal compounds[2] are commonly believed to involve a catalytically active metal imido species, involving $[2\pi + 2\pi]$ cycloaddition of the unsaturated C−C linkage across the M=N bond and subsequent protonolytic cleavage of the metallabutane/butene intermediate (Scheme 1). Originally proposed by Bergman and co-workers for intermolecular alkyne and allene HA with primary amines mediated by zirconocene compounds,[3] this mechanistic pathway was extended later to cyclohydroamination.[2e,f] Various experimental[4] and computational[5a,d,e,6] mechanistic studies have substantiated this mechanism.

Cationic group 4 metal precatalysts,[7] on the other hand, are likely to follow a different pathway (Scheme 2, cycle B) proceeding through a metal amido species, involving insertion of the unsaturated C−C linkage into the metal−amido σ bond (**3**·S → **4**·S), followed by metal−C bond aminolysis (**4**·S → **5**),[5c] reminiscent of the mechanism established for rare-earth-element catalysts.[1k,8] Compelling evidence for the operation of a metal−N σ-insertion mechanism for aminoalkene HA by charge-neutral zirconium complexes has been provided.[9] It is worth noting that cycloaddition and σ-insertive mechanisms are

Received: December 23, 2011
Published: February 28, 2012

   dx.doi.org/10.1021/ic202753m | Inorg. Chem. 2012, 51, 3786−3795

Scheme 1. Plausible Mechanistic Pathways for Early-Transition-Metal-Catalyzed Intramolecular Aminoalkene HA Proceeding through a M═NR Intermediate, Exemplified for Bis(ureate)Zr(NHR)$_2$(NH$_2$R) (3·S) as the Active Catalyst Species and Aminoalkene 1 ([Zr] = Bis(ureate)Zr)

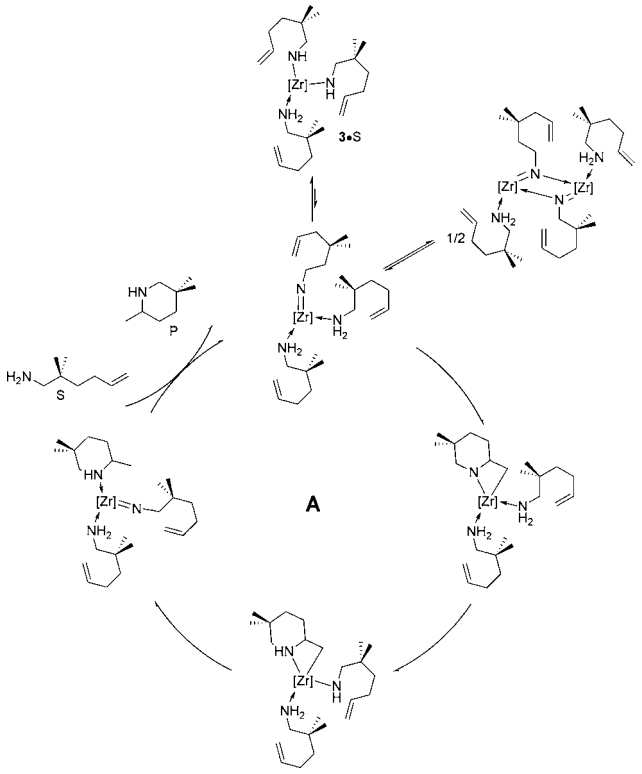

found to be energetically almost equivalent for the zirconocene-mediated HA of aminoallenes.[5e]

On the basis of observed large primary kinetic isotope effects (KIEs) of *N*-proteo- versus *N*-deuteroaminoalkene substrates in organolanthanide-catalyzed HA, together with substantial evidence for turnover-limiting olefin insertion into the Ln−C bond, a proton-assisted insertion mechanism was originally suggested[8] and the mechanistic detail was refined later as proceeding through a multicenter transition-state (TS) structure that constitutes concomitant C−N bond formation and aminolysis (Scheme 2, cycle C).[9,10] In contrast to the σ-insertive mechanism, delivery of a amino proton activates primarily the C═C linkage to undergo concurrent N−C ring closure. Hence, close proximity of the C═C linkage and the metal is no longer required. The noninsertive mechanism gives rise to cycloamine products in a single step commencing from a metal−amido substrate adduct (**3**·S). Computational studies demonstrated that the noninsertive pathway cannot compete energetically with the σ-insertive mechanism in Cp*$_2$Ln-(NHR)-catalyzed cyclization of aminodienes[11a] and amino-allenes[11b] but indicated that it may be operational for tailored catalysts with sterically demanding ligand architectures. A concerted N−C/C−H bond-forming mechanism was suggested for cyclopentadienylbis(oxazolinyl)boratezirconium-(IV)[12] and cyclopentadienylsalicyloxazolinezirconium(IV) complexes[4f] but discarded for the latter in favor of a cycloaddition mechanism, and also it was suggested for some alkali-earth-metal[13] and rare-earth-metal[14] catalysts. It is worth noting that a recent computational study[15] described the

Scheme 2. Plausible Mechanistic Pathways for Early-Transition-Metal-Catalyzed Intramolecular Aminoalkene HA Proceeding through a M−(NHR)$_2$ Intermediate, Exemplified for 3·S as the Active Catalyst Species and Aminoalkene 1 ([Zr] = Bis(ureate)Zr)

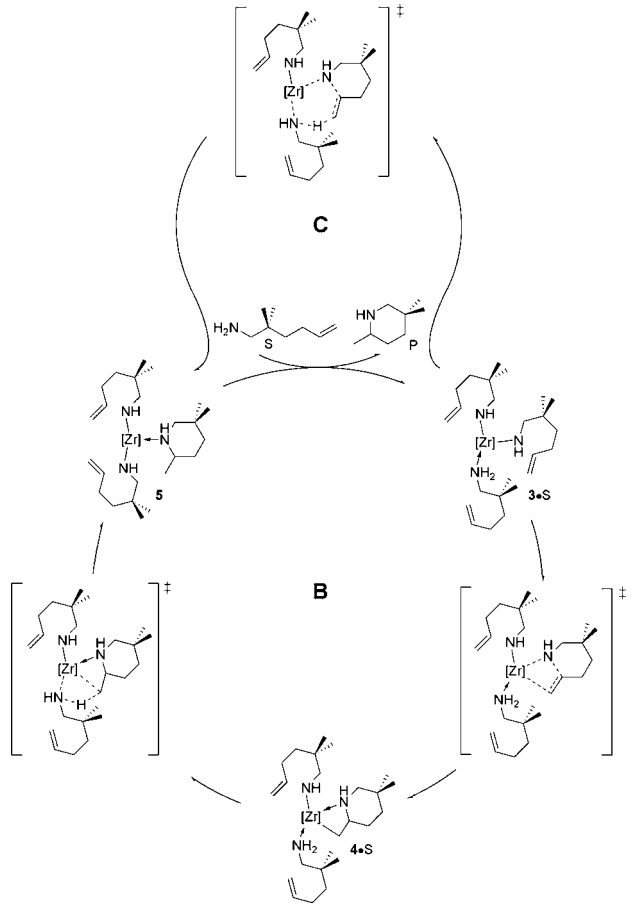

noninsertive mechanism as a viable mechanistic alternative for alkali-earth-metal-catalyzed aminoalkene HA but concluded that a σ-insertive mechanism prevails for a tris(oxazolinyl)-boratemagnesium(II) catalyst.[13a]

Recently, Schafer et al. reported a tethered bis(ureate)-Zr^{IV}(NMe$_2$)$_2$(HNMe$_2$) (**2**) compound as a competent precatalyst for intramolecular HA of both the primary and secondary 2,2-disubstituted aminoalkenes (Scheme 3).[16] In contrast to what is commonly observed, two distinct kinetic

Scheme 3. Intramolecular HA of 2,2-Disubstituted Aminoalkenes Mediated by 2

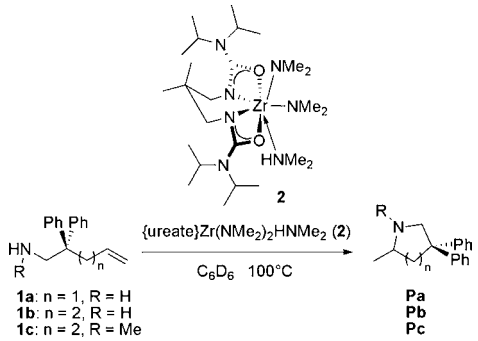

dx.doi.org/10.1021/ic202753m | *Inorg. Chem.* 2012, 51, 3786−3795

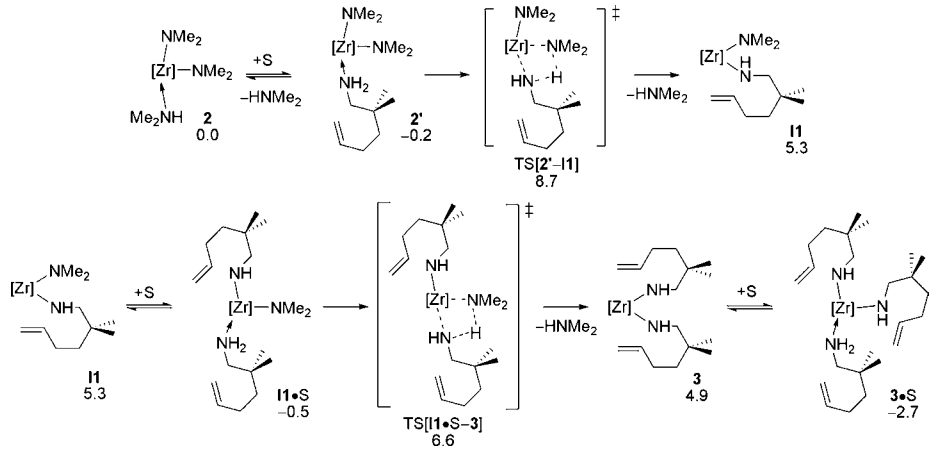

Figure 1. Consecutive Zr–NMe_2 bond aminolysis in **2** by substrate **1** ([Zr] = bis(ureate)Zr).[19a].

regimes operate, depending upon the extent of the reaction; at low conversion, the reaction rate displays first- and zero-order dependence in [catalyst] and [substrate], while a first-order dependence on the concentrations of both catalyst and substrate occurs at high conversion or alternatively with the addition of excess 2-methylpiperidine. Notably, there is no indication of the occurrence of competitive product inhibition. A mechanistic pathway proceeding through a Zr=NR intermediate (Scheme 1) has safely been discarded because **2** catalyzes the cyclization of both the primary and secondary aminoalkene substrates, together with the apparent inability of related zirconium imido compounds toward stoichiometric cycloaddition.[16] Instead, all data suggest that a zirconium(IV) bis(amido) species is the catalytically relevant intermediate. A substantial KIE of α-NH versus α-ND substitution on cyclization rates, together with reactivity trends observed for particular precatalysts, all of which are indicative of a turnover-limiting step that involves N–H bond cleavage and that requires participation of another substrate molecule led Schafer and co-workers to suggest the operation of the noninsertive pathway (Scheme 2, cycle C).[16] It should be noted that a σ-insertion mechanism featuring fast reversible insertive cyclization linked to turnover-limiting Zr–C bond aminolysis (Scheme 2, cycle B) does equally account for the observed reactivity and kinetic profiles and thus is plausible as well.[17] As aforementioned, a computational perusal of the two scenarios revealed that the σ-insertive pathway prevails for aminoalkene HA by a tris(oxazolinyl)boratemagnesium(II) catalyst.[15]

In light of the remaining uncertainty as to which of the two pathways of Scheme 2 operates, we employed density functional theory (DFT) as an established and predictive method; its particular value for unveiling mechanistic intricacies in group 4 metal-assisted HA has been demonstrated.[5,6] This study reports the comprehensive scrutiny of the intramolecular HA of prototype 2,2-dimethyl-5-penten-1-amine aminoalkene substrate **1** (S) by **2** without imposing structural simplification on any of the involved key species. The employed DFT methodology (dispersion-corrected B97-D3 functional in conjunction with basis sets of triple-ζ quality; see the Computational Methodology section) simulated authentic reaction conditions adequately, and mechanistic discussions were based on the Gibbs free-energy profiles.

Herein sound evidence is presented for the operation of a noninsertive mechanism that involves a single-step amidoalkene → cycloamine conversion through a six-center TS structure featuring N–C ring closure concomitant with amino proton delivery at the C=C bond, thereby complementing a recent experimental study.[16] The present study reveals that the identity of the catalyst resting state depends upon the relative amounts of substrate and product, thus rationalizing the two operational kinetic regimes. The proposed scenario is consonant with the observed reactivity and kinetic profiles and accounts for the large primary KIEs measured. An alternative pathway that entails reversible turnover-limiting olefin insertion into the Zr–N amido σ bond and subsequent highly exergonic Zr–C azacycle tether aminolysis is found to be not practicable and is incompatible with experimental data.

RESULTS AND DISCUSSION

An initial assessment examines the likelihood of transforming starting material **2** into the catalytically relevant $Zr(NHR)_2$ intermediate or an alternative Zr(NR) compound. Key features of the Zr–N amido stepwise σ-bond insertive and concerted noninsertive pathways of Scheme 2 are discussed next, and the two mechanisms are compared and contrasted thereafter. The accessibility of the Zr center is a crucial aspect in the control of which pathway dominates. The aptitude for substrate (S) and cycloamine (P) binding has thus been probed explicitly for each intermediate involved.

Catalyst Initiation. An effective HA requires the initial smooth conversion of starting material **2** into the $Zr(NHR)_2$ compound. Figure 1 collates the assessed energy profile for consecutive Zr–NMe_2 bond aminolysis by substrate S. The initial amine exchange[18] is almost thermoneutral, and Zr–N bond protonolysis at **2′** occurs preferably at an equatorial amido ligand evolving through a metathesis-type TS[**2′–I1**] that decays thereafter into a mixed bis(amido)zirconium(IV) intermediate **I1**. Another substrate molecule binds easily at the Zr center in **I1**, and TS[**I1**·S–**3**] traversed thereafter describes the protonolytic displacement of the second equatorial NMe_2 ligand. Facile liberation of dimethylamine affords zirconium bis(amidoalkene) **3**, to which another substrate molecule readily binds.[18] Figure 1 reveals modest barriers of 8.7 and 6.6 kcal mol^{-1} (relative to the entrance channel) for the consecutive aminolysis steps, thereby characterizing conversion of **2** into the $Zr(NHR)_2$ catalyst complex as a highly facile transformation that is, furthermore, moderately exergonic.

Zirconium Bis(amidoalkene) Compound. The catalytically relevant zirconium bis(amidoalkene) compound can be

dx.doi.org/10.1021/ic202753m | Inorg. Chem. 2012, 51, 3786–3795

present in various forms. The favorable substrate-free species **3** features two monohapto-ligated amidoalkene units. Isomer **3″**, in which one amidoalkene forms a weak chelate by orienting its double bond proximal to the metal center, is found somewhat higher in energy, while an isomer with two chelating olefin moieties could not be located (Figure 2). As was already

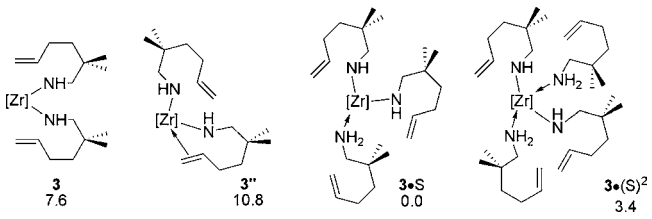

Figure 2. Various forms of the catalytically relevant bis(ureate)Zr-$(NHR)_2$ compound ([Zr] = bis(ureate)Zr).[19b].

indicated by the established structure of seven-coordinate **2**,[20] coordinative unsaturation favors the bonding of additional substrate molecules at **3**. Species with one (**3**·S) or two [**3**·$(S)^2$] adducted substrate molecules featuring monohapto Zr−N ligated amido/aminoalkene moieties have been located. The most stable **3**·S and **3**·$(S)^2$ isomers avoid an electronically disfavored trans arrangement of the two amido donor ligands, with the minimum-energy **3**·S species having as in **2** the amine bound in an axial position (Figure 2). Notably, an olefin moiety cannot compete for coordination to zirconium with an amine N-donor center either in six-coordinate **3** or in seven-coordinate **3**·S. In accordance with experimental findings,[16] DFT predicts that the catalytically competent zirconium bis(amidoalkene) compound is predominantly present as adduct **3**·S upon entry to the catalytic manifold, together with less populated **3** and **3**·$(S)^2$ species, all of which are expected to be involved in rapid amine association/dissociation equilibria.[18]

Although confidently ruled out as a catalytically relevant intermediate,[16] it is perhaps instructive to evaluate at what energy costs the related zirconium imidoalkene complex is accessible. The α abstraction of amine[21] from **3** has been studied with or without substrate participation and is found to be most favorable commencing from **3**·S (see Figure S1 in the Supporting Information). The conversion of **3**·S into substrate-adducted zirconium imido intermediate **6**·$(S)^2$ has a substantial activation energy of 28.3 kcal mol^{-1}, which exceeds the turnover-limiting barrier for productive HA catalysis (see below) and, moreover, strongly favors **3**·S.[22] It seems to disqualify any involvement of imido species for HA catalysis in the present system, thereby paralleling experiment.

***σ*-Insertive Mechanism.** The insertive pathway (Scheme 2, cycle B) that involves migratory olefin insertion into the Zr−N amido σ bond with ring closure at **3** or its substrate adducts and subsequent Zr−C azacycle tether aminolysis by a metal-adducted substrate molecule is examined first. The feasible insertive cyclization necessitates a close interaction of the olefin moiety with the metal center to ensure its proper activation toward a nucleophilic amido approach. Hence, the accessibility of the Zr center for the olefin may largely determine at which $Zr(NHR)_2$ species σ-insertive cyclization favorably proceeds.

Migratory Olefin 1,2-Insertion into the Zr−N Amido σ Bond. Various trajectories for insertive cyclization commencing from **3** and **3**·S have been examined; a TS structure of reasonably low energy with two adducted substrate molecules could not be located. An approach to the Zr center by the double bond at an axial position, hence trans to the second amido ligand (Scheme 4), describes the favorable trajectory for

Scheme 4. Alternative Trajectories for *σ*-Insertive Cyclization in 3 and 3·S

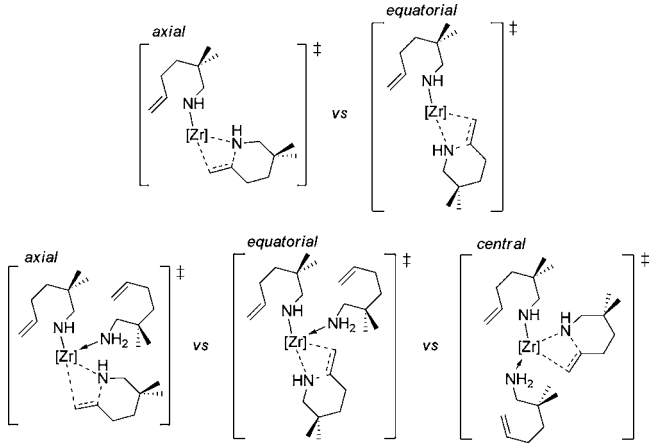

N−C ring closure at **3**.[22] It evolves through a four-center TS structure (TS[**3**−**4**]) constituting the metal-assisted olefin insertion into the Zr−N amido σ bond that occurs at a distance of 1.98 Å for the emerging C−N bond (Figure 3). Notably, an

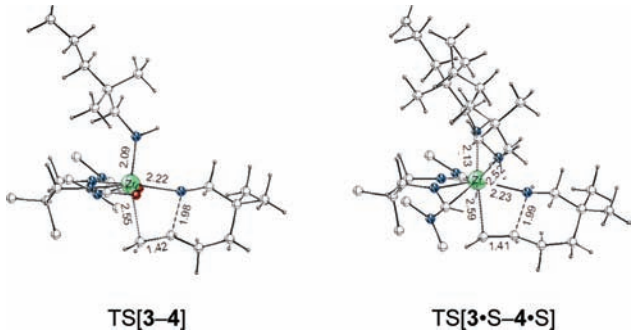

Figure 3. Located TS structure for olefin insertion into the Zr−N amido σ bond through pathways without and with participation of an adducted substrate molecule.[23]

alternative trajectory involving species with two axially bound amido units where the olefin approaches an equatorial position (Scheme 4) is found to be only marginally disfavored energetically.[22] Of the several pathways with an adducted substrate molecule scrutinized (Scheme 4, bottom), the one featuring an axial olefin approach with an equatorially bound spectator amine molecule appears to be the most accessible.[22] The connected TS[**3**·S−**4**·S] bears great similarity to TS[**3**−**4**] with regard to major structural aspects, despite some structural relaxation around the Zr center in the formally eight-coordinate TS[**3**·S−**4**·S] (Figure 4).

Figure 4 collates the assessed energy profiles for the most accessible trajectories and reveals that pathways without and with an adducted substrate molecule are virtually identical energetically. The rather marginal deviation in terms of the activation barrier ($\Delta\Delta G^{\ddagger}$ = 0.9 kcal mol^{-1}) and the thermodynamic driving force ($\Delta\Delta G$ = 0.6 kcal mol^{-1}) makes any clear decision as to which pathway prevails impossible.[24] Given that a pathway that involves an initial substrate

dx.doi.org/10.1021/ic202753m | Inorg. Chem. 2012, 51, 3786−3795

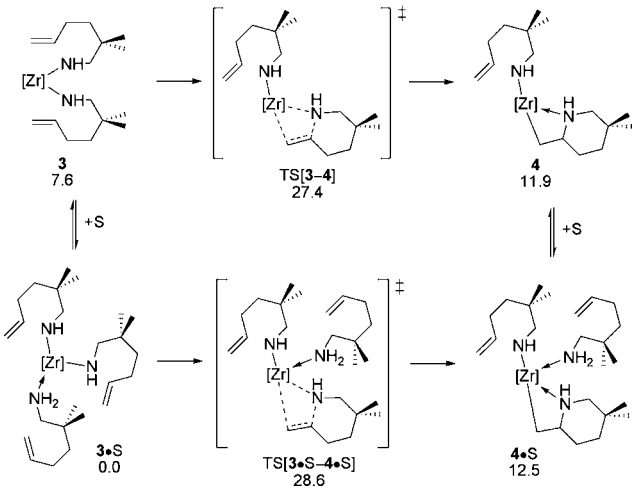

Figure 4. Migratory olefin insertion into the Zr−N amido σ bond at **3** and its substrate adducted species **3**·S ([Zr] = bis(ureate)Zr).[19b]

dissociation from **3**·S combined with substrate reassociation after cyclization is completed [**3**·S → **3** (+S) → **4** (+S) → **4**·S] is indicated not to be noticeably more facile than **3**·S → **4**·S, the latter pathway appears to be the more probable scenario. The **3**·S → **4**·S σ-insertive cyclization commencing from prevalent precursor **3**·S has an activation barrier of 28.3 kcal mol^{-1} to overcome and gives rise to a substrate-adducted azacycle intermediate **4**·S that is 12.5 kcal mol^{-1} higher in energy than **3**·S (Figure 4). It characterizes insertive ring closure as a kinetically affordable, although somewhat demanding, reversible step that favors precursor **3**·S.

Zr−C Azacycle Tether Aminolysis. After **3**·S → **4**·S insertive ring closure via the favorable trajectory shown in Figure 4 is successfully achieved, the generated substrate-adducted azacycle intermediate **4**·S featuring equatorially and axially bound substrate and alkyl moieties, respectively, is suitably set up to undergo Zr−C bond aminolysis. The minimum-energy pathway sees an initial transformation of **4**·S into a slightly less stable isomer **4′**·S through a kinetically easy azacycle rotation around the Zr−alkyl bond.[18b] Aminolysis evolves thereafter through a metathesis-like TS structure (TS[**4′**·S−**5**]; Figure 5) that describes the cleavage of an already suitably polarized N−H bond and concurrent C−H bond formation. As shown in Figure 6, the most accessible trajectory involves protonolytic cleavage of an axial Zr−C bond by an equatorially bound substrate molecule and has an activation barrier of 22.2 kcal mol^{-1}. An alternative trajectory that includes species with alkyl and amine units bound at equatorial and axial sites (Scheme 5), respectively, is found to be slightly disfavored on both kinetic and thermodynamic grounds.[22] Passage through TS[**4′**·S−**5**] affords the zirconium bis(amidoalkene)−cycloamine intermediate **5** with an axially bound piperidine molecule. Given that the N−H bond is more acidic than the C−H bond, it comes as no surprise that **4′**·S → **5** azacycle tether aminolysis is strongly downhill.

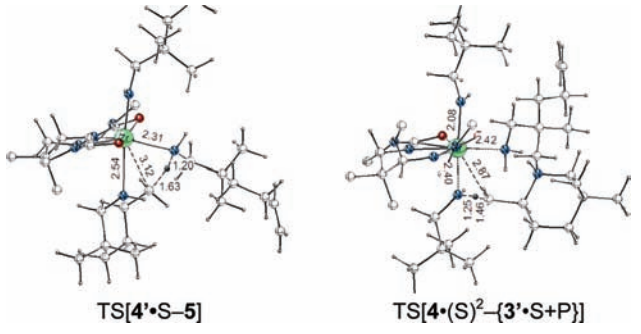

Figure 5. Located TS structure for protonolytic Zr−C azacycle bond cleavage through pathways with one or two adducted substrate molecules involved.[23]

Several trajectories for pathways with another substrate molecule involved as a spectator ligand have been examined; the most accessible one is shown in Figure 6. Association of another substrate molecule to formally eight-coordinate **4**·S comes at the expense of a disrupted Zr←N(azacycle) interaction. Notably, eight-coordinate **4**·(S)^2 and **4**·S are almost equal in energy, but Zr−C bond aminolysis commencing from **4**·(S)^2 is less probable because association of another substrate molecule destabilizes the TS structure (Figure 6). Given that the azacycle is exclusively bound via its alkyl tether to Zr in the TS structure, its decay regenerates **3**·S with liberation of piperidine product P.

Noninsertive Mechanism. This section analyzes the mechanistic pathway C in Scheme 2 that describes N−C ring closure triggered by concurrent amino proton delivery at the C═C linkage, thereby enabling amidoalkene → cycloamine transformation in a single step. The two trajectories shown in Figure 7 involve N−C ring closure at an equatorial Zr−N amido σ bond triggered by a proton delivered from an axially bound substrate via TS[**3**·S−**5′**], while TS[**3′**·S−**5**] describes concomitant ring closure at an axial Zr−N bond and proton transfer from an equatorially bound substrate molecule. The assessed energy profile indicates that the two trajectories are equally viable but with the latter traversed with a higher probability. Commencing from **3**·S, an isomeric form **3′**·S with an equatorially bound substrate molecule is readily accessible (presumably via dissociative **3**·S → **3** (+S) → **3′**·S substrate exchange),[18] and concerted amidoalkene → cycloamine conversion evolves through a six-center TS structure that constitutes N−C^6 bond formation with concurrent proton transfer from a zirconium-coordinated, and hence acidified, substrate molecule at the adjacent olefin−C^7 center. The located TS[**3′**·S−**5**] features almost complete ring closure (N−C^6 bond distance of 1.83 Å) taking place outside of the immediate metal vicinity, as indicated by a rather long Zr−C^7 distance of 3.77 Å (compared to TS[**3**·S−**4**·S] for σ-insertive cyclization; Figure 3), together with vanishing N−H (1.21 Å) and emerging C−H (1.64 Å) bonds, indicative of a nearly half-complete proton transfer (Figure 8). TS[**3′**·S−**5**] decays thereafter into a zirconium bis(amidoalkene)−cycloamine species **5** with an axially bound piperidine molecule P.

The direct conversion of **3**·S into **5** preferably proceeds through an ordered six-center TS structure (TS[**3′**·S−**5**]; Figure 8) describing concerted N−C bond formation at an equatorial Zr−N amido σ bond triggered by proton transfer from an axially bound substrate molecule. The most accessible **3′**·S → **5** trajectory has an assessed barrier of 24.3 kcal mol^{-1} to overcome and gives rise to the prevalent isomer of **5** with an axially bound cycloamine product P in a process that is driven by a large thermodynamic force (ΔG = 12.0 kcal mol^{-1}). Thus, the kinetically affordable proton-triggered noninsertive cyclization is irreversible. Given that a TS structure of reasonably low energy with two adducted substrate molecules could not be

dx.doi.org/10.1021/ic202753m | Inorg. Chem. 2012, 51, 3786−3795

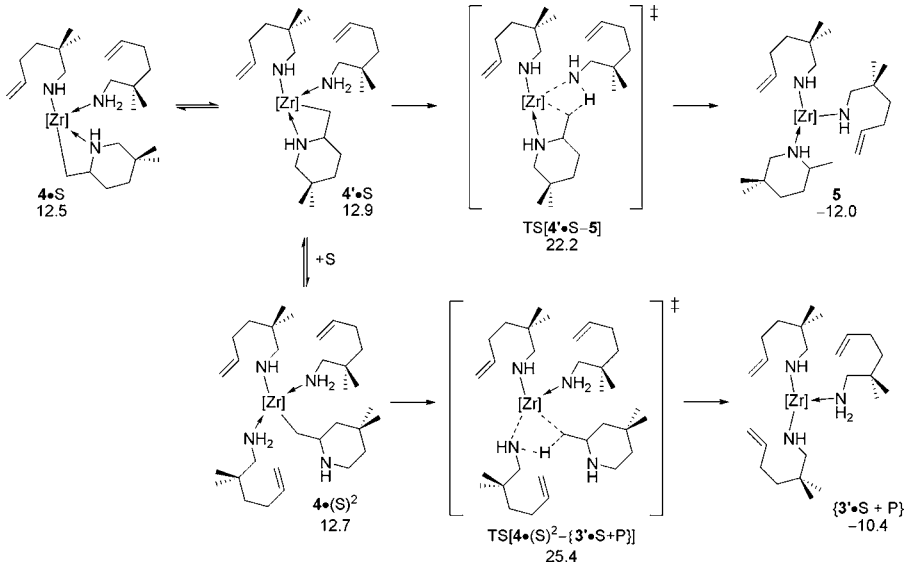

Figure 6. Zr–C azacycle tether aminolysis at **4**·S ([Zr] = bis(ureate)Zr).[19b]

Scheme 5. Alternative Trajectories for Zr–C Bond Aminolysis at 4·S

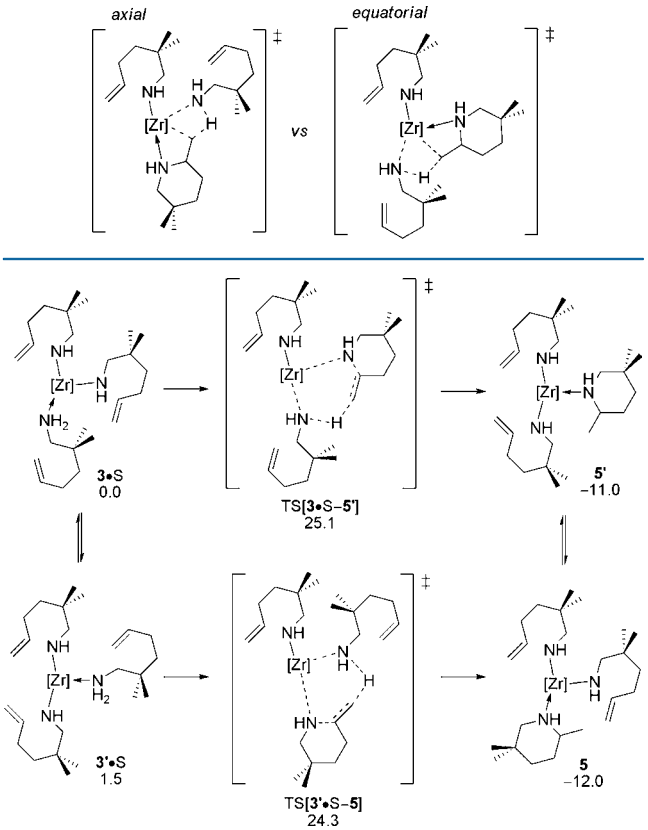

Figure 7. Noninsertive N–C ring closure with concurrent amino proton delivery at the olefin unit at **3**·S ([Zr] = bis(ureate)Zr).

located, additional substrate molecules are unlikely to accelerate the process.

Comparison of Mechanistic Pathways. This section compares and contrasts the mechanistic alternatives shown in Scheme 2. The assessed free-energy profiles for σ-insertive (right) and noninsertive (left) mechanistic pathways collated in Figure 9 reveal that the classical σ-insertive mechanism is more demanding energetically than the noninsertive pathway for intramolecular HA of aminoalkene **1** by a bis(ureate)Zr-$(NHR)_2(NH_2R)$ catalyst. The σ-insertive pathway involves a barrier of 28.3 kcal mol^{-1} for turnover-limiting reversible migratory olefin insertion into the Zr–N amido σ bond, followed by a more facile Zr–C azacycle tether aminolysis. Although it agrees with the first- and zero-order rate dependences in [catalyst] and [substrate] observed at low conversion,[16] the noncompetitive kinetic demands, together with the incompatibility of a turnover-limiting insertion step with the observed pronounced KIEs, strongly militate against the operation of the σ-insertive mechanism.

On the other hand, noninsertive cyclization through a six-center TS structure for N–C ring closure at an axial Zr–N amido σ bond triggered by concomitant proton delivery from an equatorially bound substrate molecule has a total barrier of 24.3 kcal mol^{-1}. The magnitude of the predicted kinetic gap ($\Delta\Delta G^{\ddagger}$ = 4.0 kcal mol^{-1}; Figure 9) between turnover-limiting events of the two rival mechanistic pathways provides some confidence that the noninsertive pathway prevails for the herein studied catalyst. DFT estimates a classical KIE of 3.3 to be associated with TS[**3**'·S–**5**].[26] Taking tunneling into account,[26b] one obtains a primary KIE of 3.5, pleasingly close[26d] to the experimental value of 2.9 ± 0.2 for 2,2-diphenyl-substituted 5-aminoalkene S'.[16] The direct amidoalkene → cycloamine conversion evolving through TS[**3**'·S–**5**] is strongly downhill and hence irreversible. Expulsion of an axially bound piperidine P from seven-coordinate **5** is supposedly facile[18] and most likely proceeds via dissociative **5** → **3** → **3**·S amine exchange (see Figure S6 in the Supporting Information). As an intriguing feature of the studied system, DFT predicts constants of very similar magnitude for substrate and product binding in **3**·S and **5**, respectively. Hence, dissociative **5** → **3** → **3**·S amine exchange to regenerate the catalytically relevant **3**·S intermediate is thermoneutral (Figure 9). As a further consequence, the identity of the catalyst resting state is likely to depend upon the extent of the reaction. At a primary stage of the reaction, which sees a high substrate but low product population, **3**·S likely corresponds to the catalyst resting state. Product-forming irreversible noninsertive cyclization commencing from **3**·S gives intuitively a rise to the empirical rate law of eq 1 observed

dx.doi.org/10.1021/ic202753m | Inorg. Chem. 2012, 51, 3786–3795

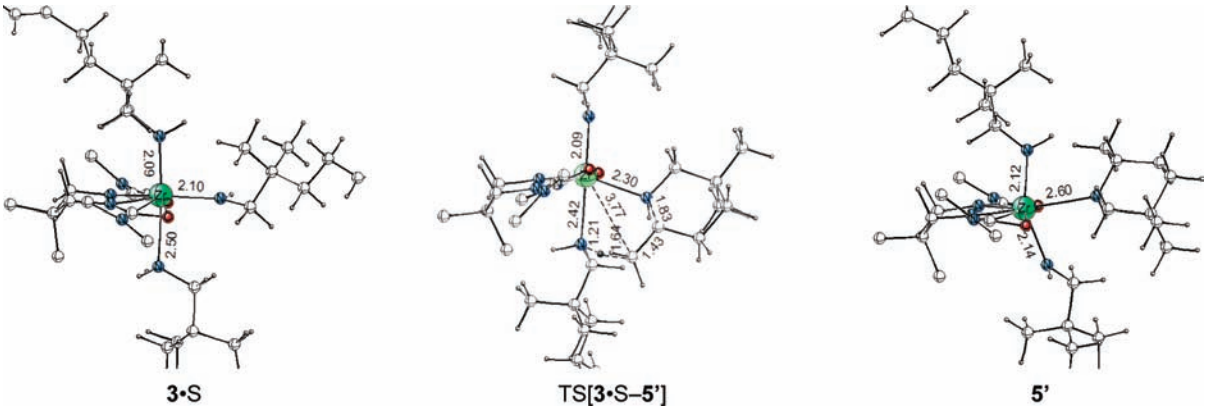

Figure 8. Selected structural parameter (angstroms) of the optimized structures of key stationary points for noninsertive N–C ring closure with concurrent amino proton transfer at the double bond in **3**·S.[23]

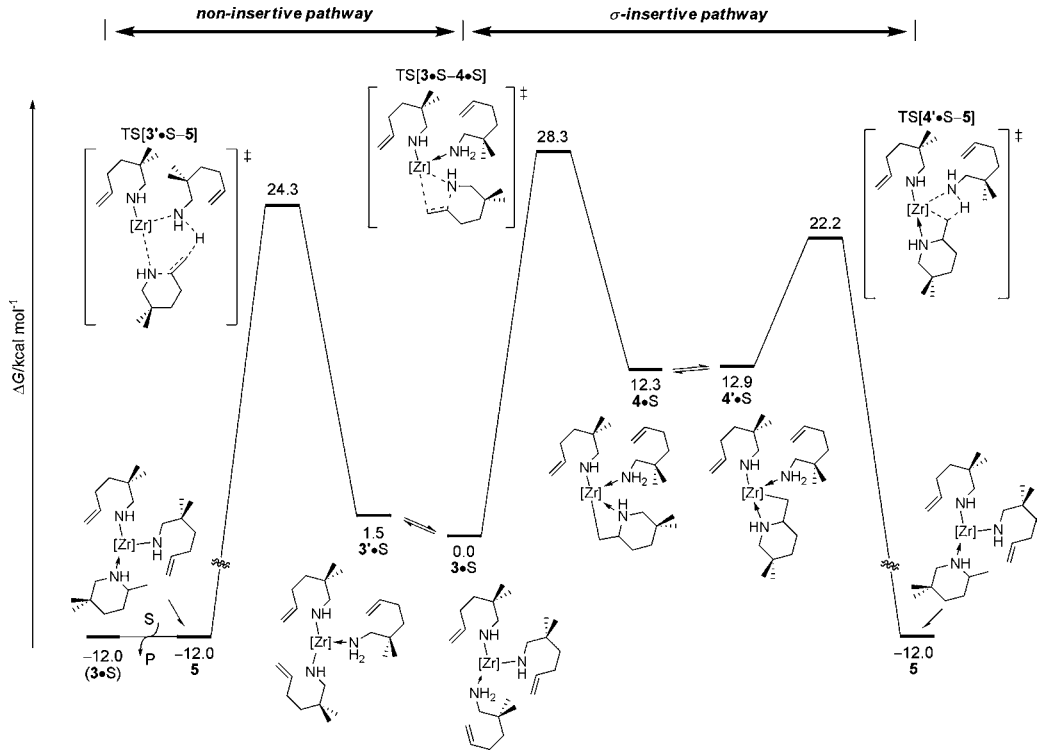

Figure 9. Overall reaction profile for intramolecular HA of aminoalkene **1** by bis(ureate)Zr(NHR)$_2$(NH$_2$R) catalyst species **3**·S proceeding via alternative mechanistic pathways. Piperidine product liberation through **5** + S → **3**·S + P is included ([Zr] = bis(ureate)Zr).

under such conditions.[16] In contrast, **5** is likely to become the catalyst resting state at high conversion or alternatively with the addition of excess 2-methylpiperidine. Simple kinetic modeling for this scenario gives rise to the second-order empirical rate law of eq 2, which reflects the observed other kinetic regime. The unique comparable binding strength of the substrate and cycloamine in **3**·S and **5**, resulting in a facile **5** ⇆ **3** ⇆ **3**·S dissociative equilibrium that favors either side depending on the relative populations of S and P, explains the operation of two kinetic regimes based on the change of the catalyst resting state's identity and its observed almost identical rates.

$$\nu \sim [\text{catalyst}]^1[\text{substrate}]^0 \quad (1)$$

$$\nu \sim [\text{catalyst}]^1[\text{substrate}]^1 \quad (2)$$

Equilibrium between Zirconium Piperidine and Zirconium Piperide Compounds. Dissociative substitution of P by S at **5** regenerates the catalytically relevant intermediate **3**·S and liberates the product. However, the acidified piperidine N–H is also susceptible to α-proton abstraction, which transforms **5** into a zirconium piperide–amidoalkene–aminoalkene intermediate **7**. An equilibrium between the primary and secondary amido species that may favor the latter has been discussed in the context of product inhibition observed at increasing conversion.[25] The energy profiles collated in Figure 10 (note that the free energy of S → P conversion has been subtracted where appropriate) characterize the H$^+$ exchange between amidoalkene and piperidine units at **5** as a kinetically easy, reversible process that favors **5**. Not only are the substrate and cycloamine products bound at comparable strength (similar binding properties) in **3**·S and **5** (see Figure 9), secondary

dx.doi.org/10.1021/ic202753m | Inorg. Chem. 2012, 51, 3786–3795

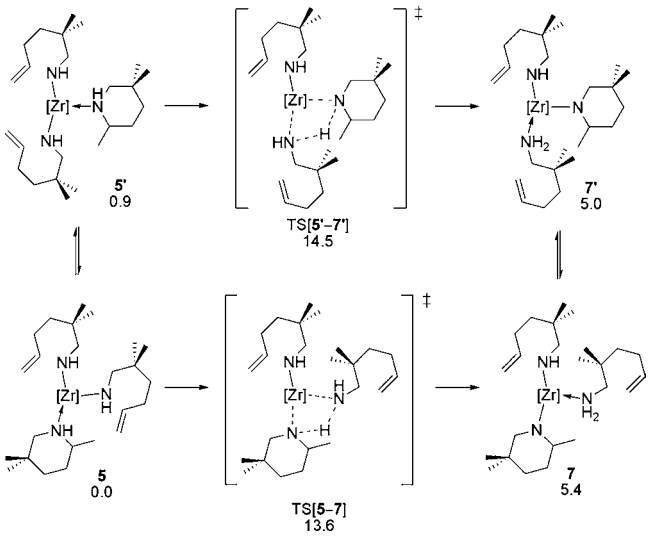

Figure 10. H^+ exchange between amido and piperidine units at **5** ([Zr] = bis(ureate)Zr).[19b,c]

amido species are also disfavored thermodynamically relative to related primary amido species. Accordingly, in consonance with experimental findings,[16] competitive product inhibition is unlikely to be of relevance for the present catalyst system.

Aptitude of Various Zirconium Amidoalkene–Amine Species for Noninsertive Ring Closure. Another intriguing aspect that needs to be addressed is the likelihood of the various zirconium amidoalkene species bearing an acidified amine N–H functionality traversing the operative noninsertive pathway. The assessed energy profiles for proton-triggered cyclization at intermediates **5** and **7** and zirconium piperide–amido–piperidine species **8**, which results from cyclization at **5**, can be found in Figures S8–S10 in the Supporting Information). As a common aspect, all intermediates favor a trajectory identical with that of **3′**·S → **5** in Figure 7 on both kinetic and thermodynamic grounds. However, the kinetic demands (which is most conveniently discussed in terms of normalized barriers)[19c] are markedly different for the various intermediates, of which **5** exhibits the smallest barrier of 27.0 kcal mol^{-1}. Given that cyclization at **5** is triggered by a piperidine N–H instead of a more acidic amidoalkene N–H as in **3**·S, the slower **5** → **8** cyclization becomes understandable. The predicted kinetic gap of 2.7 kcal mol^{-1} ($\Delta\Delta G^{\ddagger}$) between **3**·S → **5** and **5** → **8** pathways indicates a probability ∼100 times lower for traversing the latter, and hence noninsertive cyclization at **5** appears not to be competitive with the **3**·S → **5** pathway for productive HA catalysis. Although of minor mechanistic relevance, a piperidine α-proton abstraction that is sufficiently facile and far on the left transforms **8** into zirconium dipiperide–aminoalkene intermediate **9** (see Figure S5 in the Supporting Information). Besides the acidity of the N–H functionality, spatial demands of amine and amido ligands also have a profound impact on the kinetics. The substitution of an acyclic amidoalkene (**3**·S) by a bulkier piperide (**7**) increases the barrier by 4.0 kcal mol^{-1} ($\Delta\Delta G^{\ddagger}$ for **3**·S → **5** versus **7** → **8**) and a similar behavior is seen for **5** → **8** versus **8** → **10** ($\Delta\Delta G^{\ddagger}$ = 4.7 kcal mol^{-1}) piperidine N–H-triggered cyclizations.[22] This leads to the conclusion that zirconium amidoalkene species with piperidine and/or piperide ligands remain inactive toward cyclization; hence, intermediates like **7**–**10** have no anticipated role in HA catalysis by the present system. Also noteworthy is that the presence of a bulky piperide ligand favors a six-coordinate zirconium diamido intermediate involved in dissociative product displacement (see Figure S7 in the Supporting Information) compared to product expulsion from **5** (see Figure S6 in the Supporting Information), but it has little mechanistic implication.

CONCLUSION

The present study aims to contribute toward a more detailed mechanistic understanding of the intramolecular HA of aminoalkenes by a tethered bis(ureate)$Zr^{VI}(NMe_2)_2(HNMe_2)$ starting material **2**. This employs DFT as an established and predictive method to scrutinize rival mechanistic pathways that proceed through a $Zr(NHR)_2$ intermediate. The classical stepwise σ-insertive mechanism that involves migratory olefin insertion into the Zr–N amido σ bond with ring closure and subsequent Zr–C azacycle tether aminolysis has been compared with a pathway for single-step amidoalkene → cycloamine conversion through N–C ring closure concurrent with amino proton transfer at the adjacent olefin–C center. The noncompetitive kinetic demands for endergonic, hence reversible, σ-insertive cyclization linked to a more facile Zr–C bond aminolysis, together with the incompatibility of a turnover-limiting insertion step with the observed large primary KIEs, strongly militate against the operation of an σ-insertive mechanism. Computational analysis of the intramolecular HA of prototype aminoalkene **1** by **2** corroborates a recent experimental study[16] that was suggestive of a concerted proton-assisted cyclization pathway. The noninsertive cyclization that commences from a catalytically relevant seven-coordinate $Zr^{IV}(NHR)_2(NH_2R)$ substrate adduct **3**·S through a six-center TS structure describing N–C ring closure at an axial Zr–N amido σ bond triggered by concurrent proton delivery from an equatorially bound substrate molecule is found to be energetically superior; its effective barrier assessed by DFT compares reasonably well with empirically determined Eyring parameters,[16b] and the computationally estimated primary KIEs match the observed values pleasingly well. The direct amidoalkene → cycloamine transformation is strongly downhill, hence irreversible, and product expulsion from seven-coordinate **5** by the substrate most likely proceeds via facile dissociative **5** → **3** → **3**·S amine exchange. The present study reveals that the substrate and cycloamine bind at almost equivalent strengths in **3**·S and **5**, together with a rapid equilibrium between primary and secondary amido species that is far on the left, which are unique features of the studied catalyst. These findings indicate that **3**·S corresponds to the catalyst resting state at high substrate concentration, while it becomes **5** when the product concentration is high or with the addition of excess 2-methylpiperidine, and this ambivalent behavior rationalizes the observed operation of two distinct kinetic regimes, depending upon the extent of the reaction.[16] As a further implication, competitive product inhibition can likely be discarded, as was found experimentally.[16] Moreover, DFT predicts that zirconium amidoalkene species with piperidine and/or piperide ligands are inactive toward proton-triggered cyclization under the given reaction conditions, thereby indicating that these species have no significant role in HA for the studied catalyst.

The computational analysis presented herein that favors the operation of a proton-triggered noninsertive mechanism for amidoalkene HA by a bis(ureate)$Zr^{IV}(NHR)_2(NH_2R)$ catalyst species complements a recent experimental study. It is

dx.doi.org/10.1021/ic202753m | *Inorg. Chem.* 2012, 51, 3786–3795

indicative that for zirconium complexes with sterically encumbering ligands architectures, like the studied bis(ureate) system, the limited access of the metal center for the olefin unit disfavors σ-insertive cyclization, thereby rendering proton-triggered noninsertive cyclization the favorable mechanistic scenario. These findings, together with valuable insights into the catalytic structure−reactivity relationships, will likely direct the rational design of group 4 metal-based catalysts and facilitate further advances in the area.

COMPUTATIONAL METHODOLOGY

All calculations based on Kohn−Sham DFT[27] were performed by means of the program package *TURBOMOLE*[28] using the dispersion-corrected B97-D functional[29] within the RI-*J* integral approximation[30] in conjunction with flexible basis sets of triple-ζ quality. Empirical dispersion corrections by Grimme (D3 with Becke−Johnson damping)[31] were used to account for noncovalent interactions; energy and gradient components were calculated with the stand-alone *dftd3* program.[31c] For zirconium, we used the Stuttgart−Dresden quasi-relativistic effective core potential (SDD)[32] with the associate (7s7p5d1f)/[6s4p3d1f] valence basis set (def2-TZVP).[33] All remaining elements were represented by Ahlrich's valence triple-ζ TZVP basis set[34] with polarization functions on all atoms. The DFT calculations have simulated the authentic reaction conditions by treating the bulk effects of the benzene solvent by a consistent continuum model in the form of the conductor-like screening model (COSMO).[35] All of the stationary points were fully located at the B97-D3 level with inclusion of solvation. Frequency calculations were performed to confirm the nature of all optimized key structures and to determine thermodynamic parameters (298 K, 1 atm) under the rigid-rotor and harmonic approximations. The mechanistic conclusions drawn in this study were based on the Gibbs free-energy profile of the entire catalytic cycle assessed at the B97-D3(COSMO)/SDD+TZVP level of approximation for experimental condensed-phase conditions. Further details are given in the Supporting Information. Calculated structures were visualized by employing the *StrukEd* program,[36] which was also used for the preparation of 3D molecule drawings.

ASSOCIATED CONTENT

Supporting Information

Figures S1−S14, Tables S1−S7, full details of the employed computational methodology, and a full account of the assessed energy profiles for all of the studied pathways. This material is available free of charge via the Internet at http://pubs.acs.org.

AUTHOR INFORMATION

Corresponding Author

*E-mail: st40@st-andrews.ac.uk.

Notes

The authors declare no competing financial interest.

REFERENCES

(1) For reviews of catalytic HA, see: (a) Hegedus, L. S. *Angew. Chem.* **1988**, *100*, 1147; *Angew. Chem., Int. Ed. Engl.* **1998**, *27*, 1113. (b) Roundhill, D. M. *Catal. Today* **1997**, *37*, 155. (c) Müller, T. E.; Beller, M. *Chem. Rev.* **1988**, *98*, 675. (d) Nobis, M.; Drießen-Hölscher, B. *Angew. Chem.* **2001**, *113*, 4105; *Angew. Chem., Int. Ed.* **2001**, *40*, 3983. (e) Taube, R. In *Applied Homogeneous Catalysis with Organometallic Complexes*; Cornils, B., Herrmann, W. A., Eds.; Wiley-VCH: Weinheim, Germany, 2002; pp 513−524. (f) Seayad, F.; Tillack, A.; Hartung, C. G.; Beller, M. *Adv. Synth. Catal.* **2002**, *344*, 795. (g) Molander, G. A.; Romero, J. A. C. *Chem. Rev.* **2002**, *102*, 2161. (h) Pohlki, F.; Doye, S. *Chem. Soc. Rev.* **2003**, *32*, 104. (i) Roesky, P. W.; Müller, T. E. *Angew. Chem.* **2003**, *115*, 2812; *Angew. Chem., Int. Ed.* **2003**, *42*, 2708. (j) Hartwig, J. F. *Pure Appl. Chem.* **2004**, *76*, 507. (k) Hong, S.; Marks, T. J. *Acc. Chem. Res.* **2004**, *37*, 673. (l) Hultzsch, K. C. *Adv. Synth. Catal.* **2005**, *347*, 367. (m) Odom, A. L. *Dalton Trans.* **2005**, 225. (n) Severin, R.; Doye, S. *Chem. Soc. Rev.* **2007**, *36*, 1407. (o) Aillaud, I.; Collin, J.; Hannedouche, J.; Schulz, E. *Dalton Trans.* **2007**, 5105. (p) Hartwig, J. F. *Nature* **2008**, *455*, 314. (q) Müller, T. E.; Hultzsch, K. C.; Yus, M.; Foubelo, F.; Tada, M. *Chem. Rev.* **2008**, *108*, 3795. (r) Reznichenko, A. L.; Hultzsch, K. C. *Top. Organomet. Chem.* **2011**, in press.

(2) For cyclohydroamination mediated by charge-neutral group 4 transition-metal complexes, see: (a) McGrane, P. L.; Livinghouse, T. *J. Org. Chem.* **1992**, *57*, 1323. (b) McGrane, P. L.; Jensen, M.; Livinghouse, T. *J. Am. Chem. Soc.* **1992**, *114*, 5459. (c) McGrane, P. L.; Livinghouse, T. *J. Am. Chem. Soc.* **1993**, *115*, 11485. (d) Bytschkov, I.; Doye, S. *Tetrahedron Lett.* **2002**, *43*, 3715. (e) Ackermann, L.; Bergman, R. G. *Org. Lett.* **2002**, *4*, 1475. (f) Ackermann, L.; Bergman, R. G. *J. Am. Chem. Soc.* **2003**, *125*, 11956. (g) Li, C.; Thomson, R. K.; Gillon, B.; Patrick, B. O.; Schafer, L. L. *Chem. Commun.* **2003**, 2462. (h) Bexrud, J. A.; Beard, J. D.; Leitch, D. C.; Schafer, L. L. *Org. Lett.* **2005**, *7*, 1959. (i) Kim, H.; Lee, P. H.; Livinghouse, T. *Chem. Commun.* **2005**, 5205. (j) Petersen, J. R.; Hoover, J. M.; Kassel, W. S.; Rheingold, A. L.; Johnson, A. R. *Inorg. Chim. Acta* **2005**, *358*, 687. (k) Heutling, A.; Pohlki, F.; Bytschkov, I.; Doye, S. *Angew. Chem.* **2005**, *117*, 3011; *Angew. Chem., Int. Ed.* **2005**, *44*, 2951. (l) Müller, C.; Loos, C.; Schulenburg, N.; Doye, S. *Eur. J. Org. Chem.* **2006**, 2499. (m) Watson, D. A.; Chiu, M.; Bergman, R. G. *Organometallics* **2006**, *25*, 4731. (n) Wood, M. C.; Leitch, D. C.; Yeung, C. S.; Kozak, J. A.; Schafer, L. L. *Angew. Chem.* **2007**, *119*, 358; *Angew. Chem., Int. Ed.* **2007**, *46*, 354. (o) Ackermann, L.; Kaspar, L. T.; Althammer, A. *Org. Biomol. Chem.* **2007**, *5*, 1975. (p) Majumder, A. L.; Odom, A. L. *Organometallics* **2008**, *27*, 1174. (q) Leitch, D. C.; Payne, P. R.; Dunbar, C. R.; Schafer, L. L. *J. Am. Chem. Soc.* **2009**, *131*, 18246. (r) Bexrud, J. A.; Schafer, L. L. *Dalton Trans.* **2010**, *39*, 361. (s) Reznichenko, A. L.; Hultzsch, K. C. *Organometallics* **2010**, *29*, 24.

(3) (a) Walsh, P. J.; Baranger, A. M.; Bergman, R. G. *J. Am. Chem. Soc.* **1992**, *114*, 1708. (b) Baranger, A. M.; Walsh, P. J.; Bergman, R. G. *J. Am. Chem. Soc.* **1993**, *115*, 2753. (c) Lee, S. Y.; Bergman, R. G. *Tetrahedron* **1995**, *51*, 5255. (d) Johnson, J. S.; Bergman, R. G. *J. Am. Chem. Soc.* **2001**, *123*, 2923.

(4) (a) Pohlki, F.; Doye, S. *Angew. Chem.* **2001**, *113*, 2361; *Angew. Chem., Int. Ed.* **2001**, *40*, 2305. (b) Li, Y.; Shi, Y.; Odom, A. L. *J. Am. Chem. Soc.* **2004**, *126*, 1794. (c) Ward, B. D.; Maisse-Francois, A.; Mountford, P.; Gade, L. H. *Chem. Commun.* **2004**, 704. (d) Thomson, R. K.; Bexrud, J. A.; Schafer, L. L. *Organometallics* **2006**, *25*, 4069. (e) Gott, A. L.; Clarke, A. J.; Clarkson, G. J.; Scott, P. *Chem. Commun.* **2008**, 1422. (f) Allan, L. E. N.; Clarkson, G. J.; Fox, D. J.; Gott, A. L.; Scott, P. *J. Am. Chem. Soc.* **2010**, *132*, 15308.

(5) For computational studies of group 4 metal-assisted intramolecular HA of various substrate classes, for aminoalkene substrates, see: (a) Müller, C.; Koch, R.; Doye, S. *Chem.—Eur. J.* **2008**, *14*, 10430. (b) Gott, A. L.; Clarkson, G. J.; Deeth, R. J.; Hammond, M. L.; Morton, C.; Scott, P. *Dalton Trans.* **2008**, 2983. For aminoallene substrates, see: (c) Tobisch, S. *Dalton Trans.* **2006**, 4277. (d) Tobisch, S. *Chem.—Eur. J.* **2007**, *13*, 4884. (e) Tobisch, S. *Chem.—Eur. J.* **2008**, *14*, 8590.

(6) Straub, B. F.; Bergman, R. G. *Angew. Chem., Int. Ed.* **2001**, *40*, 4632.

(7) For cyclohydroamination mediated by cationic group 4 metal complexes, see: (a) Gribkov, D. V.; Hultzsch, K. C. *Angew. Chem.* **2004**, *116*, 5659; *Angew. Chem., Int. Ed.* **2004**, *43*, 5542. (b) Knight, P. A.; Munslow, I.; O'Shaughnessy, P. N.; Scott, P. *Chem. Commun.* **2004**, 894. (c) Wang, X.; Chen, Z.; Sun, X.-L.; Tang, Y.; Xie, Z. *Org. Lett.* **2011**, *13*, 4748.

(8) Gagné, M. R.; Stern, C. L.; Marks, T. J. *J. Am. Chem. Soc.* **1992**, *114*, 275.

(9) Stubbert, B. D.; Marks, T. J. *J. Am. Chem. Soc.* **2007**, *129*, 6149.

(10) Allan, L. E.; Fox, D. J.; Deeth, R. J.; Gott, A. L.; Scott, P. Proceedings of the 42nd IUPAC Congress, Glasgow, U.K., Aug 2−7, 2009.

(11) (a) Tobisch, S. *Chem.—Eur. J.* **2010**, *16*, 13814. (b) Tobisch, S. *Dalton Trans.* **2011**, *40*, 249.

(12) Manna, K.; Xu, S.; Sadow, A. D. *Angew. Chem., Int. Ed.* **2011**, *50*, 1865.
(13) (a) Dunne, J. F.; Fulton, D. B.; Ellern, A.; Sadow, A. D. *J. Am. Chem. Soc.* **2010**, *132*, 17680. (b) Arrowsmith, M.; Crimmin, M. R.; Barrett, A. G. M.; Hill, M. S.; Kociak-Köhn, G.; Procopiou, P. A. *Organometallics* **2011**, *30*, 1493.
(14) Hangaly, N. K.; Petrov, A. R.; Rufanov, K. A.; Harms, K.; Elfferding, M.; Sundermeyer, J. *Organometallics* **2011**, *30*, 4544.
(15) Tobisch, S. *Eur. J. Chem.* **2011**, *17*, 14974.
(16) (a) Leitch, D. C.; Platel, R. H.; Schafer, L. L. *J. Am. Chem. Soc.* **2011**, *133*, 15453. (b) Eyring analysis for the cyclization of 2,2-diphenyl-substituted 5-aminoalkene S′ by **2** afforded $\Delta H^{\ddagger} = 20.1 \pm 0.5$ kcal mol^{-1} and $\Delta S^{\ddagger} = -21.0 \pm 1.0$ cal K^{-1} mol^{-1}; hence, $\Delta G^{\ddagger} = 26.4 \pm 0.8$ kcal mol^{-1} (298 K). Unfortunately, Eyring data have not been reported for 2,2-dimethyl-substituted 5-aminoalkene S.
(17) It should be noted, however, that β-amide elimination as the reverse of olefin insertion into the metal−N amido σ bond has not been reported thus far for group 4 metal complexes. See ref 16a for details.
(18) (a) Amine association and dissociation at the various intermediates are presumably facile, and rapid equilibria are expected. (b) Examination by a linear-transit approach gave no indication that such processes are associated with a significant enthalpic barrier.
(19) (a) The bis(ureate)$Zr^{IV}(NMe_2)_2(HNMe_2)$ **2** (with the appropriate number of substrate molecules) has been chosen as a reference for relative free energies given in kilocalories per mole. (b) The prevalent bis(ureate)$Zr^{IV}(NHR)_2(NH_2R)$ substrate adduct **3**·S, featuring monohapto Zr−N ligated amido/aminoalkene moieties, of the catalytically competent $Zr(NHR)_2$ complex (with the appropriate number of substrate or cycloamine molecules) has been chosen as a reference for relative free energies given in kilocalories per mole. (c) The reaction free energy of S → P conversion has been subtracted where appropriate.
(20) Leitch, D. C.; Schafer, L. L. *Organometallics* **2010**, *29*, 5162.
(21) (a) Walsh, P. J.; Hollander, F. J.; Berman, R. G. *Organometallics* **1993**, *12*, 3705. (b) Duncan, A. P.; Bergman, R. G. *Chem. Rec.* **2002**, *2*, 431.
(22) See the Supporting Information for further details.
(23) The isopropyl and methyl groups of the bis(ureate)zirconium backbone and also amino/amidoalkene units are displayed in a truncated fashion.
(24) (a) The computational estimation of entropies for condensed-phase conditions is an active area of ongoing research; see the Supporting Information. It thus leaves one with some ambiguity in comparing processes of different molecularity at the free-energy surface. The assessed deviation in free energy of ∼1 kcal mol^{-1} is certainly too small for any firm conclusions. (b) Note that DFT is capable of predicting the relative kinetics ($\Delta\Delta G^{\ddagger}$) of stereoisomeric pathways of a given transformation in high accuracy (of less than 1 kcal mol^{-1}). For instance, see: (c) Tobisch, S.; Ziegler, T. *J. Am. Chem. Soc.* **2002**, *124*, 13290. (d) Tobisch, S. *Chem.—Eur. J.* **2003**, *9*, 1217. (e) Tobisch, S.; Ziegler, T. *J. Am. Chem. Soc.* **2004**, *126*, 9059. (f) Tobisch, S. *Chem.—Eur. J.* **2006**, *12*, 2520.
(25) (a) Giardello, M. A.; Conticello, V. P.; Brard, L.; Gagne, M. R.; Marks, T. J. *J. Am. Chem. Soc.* **1994**, *116*, 10241. (b) Gribkov, D. V.; Hultzsch, K. C.; Hampel, F. *Chem.—Eur. J.* **2003**, *9*, 4796. (c) Bambirra, S.; Tsurugi, H.; van Leusen, D.; Hessen, B. *Dalton Trans.* **2006**, 1157.
(26) (a) The primary KIEs have been estimated from deviation of the zero-point-vibrational energies and partition function values for **1** and **1**-d_2 substrates. (b) Zero curvature tunneling has been accounted for by the Skodje and Truhlar approximation.[26c] See the Supportimg Information for details. (c) Skodje, R. T.; Truhlar, D. G.; Garrett, B. C. *J. Phys. Chem.* **1981**, *85*, 3019. (d) The accuracy of computationally predicting k_H/k_D values for hydrogen-transfer processes is limited by TS theory approximation,[26e] semiclassical tunneling corrections, and rigid-rotator harmonic oscillator approximation for vibrational frequencies. (e) Lu, D. H.; Maurice, D.; Truhlar, D. G. *J. Am. Chem. Soc.* **1990**, *112*, 6206.
(27) Parr, R. G.; Yang, W. *Density-Functional Theory of Atoms and Molecules*; Oxford University Press: Oxford, U.K., 1989.
(28) (a) Ahlrichs, R.; Bär, M.; Häser, M.; Horn, H.; Kölmel, C. *Chem. Phys. Lett.* **1989**, *162*, 165. (b) Treutler, O.; Ahlrichs, R. *J. Chem. Phys.* **1995**, *102*, 346. (c) Ahlrichs, R.; Furche, F.; Hättig, C.; Klopper, W.; Sierka, M.; Weigend, F. *TURBOMOLE*, version 6.0; University of Karlsruhe: Karlsruhe, Germany, 2009; http://www.turbomole.com.
(29) Grimme, S. *J. Comput. Chem.* **2006**, *27*, 1787.
(30) (a) Vahtras, O.; Almlöf, J.; Feyereisen, M. W. *Chem. Phys. Lett.* **1993**, *213*, 514. (b) Eichkorn, K.; Treutler, O.; Öhm, H.; Häser, M.; Ahlrichs, R. *Chem. Phys. Lett.* **1995**, *242*, 652.
(31) (a) Grimme, S.; Anthony, J.; Ehrlich, S.; Krieg, H. *J. Chem. Phys.* **2010**, *132*, 154104. (b) Grimme, S.; Ehrlich, S.; Goerigk, L. *J. Comput. Chem.* **2011**, *32*, 1456. (c) http://toc.uni-muenster.de/DFTD3/getd3.html.
(32) Andrae, D.; Häußermann, U.; Dolg, M.; Stoll, H.; Preuß, H. *Theor. Chim. Acta* **1990**, *77*, 123.
(33) (a) Weigend, F.; Ahlrichs, R. *Phys. Chem. Chem. Phys.* **2005**, *7*, 3297. (b) Weigend, F. *Phys. Chem. Chem. Phys.* **2006**, *8*, 1057.
(34) (a) Schäfer, A.; Huber, C.; Ahlrichs, R. *J. Chem. Phys.* **1994**, *100*, 5829. (b) Eichkorn, K.; Weigend, F.; Treutler, O.; Ahlrichs, R. *Theor. Chem. Acc.* **1997**, *97*, 119.
(35) (a) Klamt, A.; Schüürmann, G. *J. Chem. Soc., Perkin Trans. 2* **1993**, 799. (b) Klamt, A. In *Encyclopedia of Computational Chemistry*; Schleyer, P. v. R., Eds.; John Wiley & Sons: Chichester, U.K., 1998; Vol. *1*, pp 604−615.
(36) For further details, see: http://www.struked.de.